

Theory of Auger spectra for molecular-field-split core levels

Faris Gel'mukhanov and Hans Ågren

Institute of Physics and Measurement Technology, University of Linköping, S-58183 Linköping, Sweden

Svante Svensson

Institute of Physics, University of Uppsala, S-75121 Uppsala, Sweden

Helena Aksela and Seppo Aksela

Department of Natural Sciences, University of Oulu, FIN-90570 Oulu, Finland

(Received 21 August 1995)

A theory for nonradiative decay of molecular-field-split states is presented. It is shown that the relative inner-shell sublevel cross sections for Auger transitions are sensitively dependent on the matching of spin-orbit and molecular-field interactions. This can lead to suppression of particular sublevel Auger transitions and to a breakdown of the constant core-hole lifetime approximation. The investigated effects are caused by a strong dependence of the Auger intensity on the mutual local space orientation of initial- and final-state orbitals. These features are illustrated for S $2p$ ($L_{II,III}VV$) Auger spectra of H_2S , and explain the apparent mismatch of $2p$ spin-orbit energies observed in Auger and photoelectron spectra of this molecule.

PACS number(s): 33.80.Eh, 33.50.Hv, 33.70.Jg

I. INTRODUCTION

Over the last decade significant progress has been made in the study of core-level excitation processes with the help monochromatized high-intensity synchrotron radiation. Improved implementations of storage ring undulators has in combination with very high-resolution electron spectroscopy led to a number of new phenomena in radiative and nonradiative Raman scattering. As is well known, the assignment of nonradiative, Auger, spectra is more complex than that of the radiative counterpart because dipole selection rules governing the latter are replaced by an interelectron Coulomb interaction which is less selective and which leads to final states of higher ionicity. The interpretation of Auger and Auger Raman spectra remains a challenge also because of the coexistence of several factors that are unraveled at high resolution.

In the present work we address a particular aspect in nonradiative (Auger) Raman spectra, which also is relevant for normal Auger spectra of second- and higher-row elements, namely, the nonradiative decay from molecular-field (MF) split core-excited states. Auger spectra of hydrides have shown very interesting features, which at the same time have posed some unresolved problems and even disagreements in the interpretations. The Auger electron spectra of H_2S [1,2], HBr [3,4], and HI [5–7] are examples of this contention. The MF splitting has been resolved in the Br $3d$ core photoelectron spectrum in Ref. [3]. By using this information, an assignment has been made of the MVV spectrum of the same molecule that is in disagreement with the assignment made by the authors of Ref. [4], who based their interpretation on a vibrational analysis. The same applies also to the case of the NVV spectrum of the HI molecule, as judged by the debate in the literature [5–7]. Also some peculiar details on an apparent difference in the spin-orbit (SO) splitting of the S $2p$ level in H_2S when comparing x-ray photoelectron and Auger electron spectroscopy results have indicated that the

comparison between the spectroscopies is not straightforward [1].

The improved experimental capacity in terms of resolution and brightness of the radiation sources has now cast light on the problem of the disagreement between Auger electron spectroscopy and core photoelectron spectroscopy, as discussed above. Recently, the SO and MF splittings of the sulfur $L_{II,III}$ shell of the H_2S molecule have been studied at the molecular physics beamline (BL51, “the Finnish beamline”) at the MAX laboratory, using both x-ray photoelectron and Auger electron spectroscopy [8]. The SO interaction and MF split the $L_{II,III}$ shell into three sublevels, $3e_{1/2}$, $4e_{1/2}$, and $5e_{1/2}$. While all three sublevels are seen with comparable intensities in the x-ray photoelectron spectrum (XPS), only $3e_{1/2}$ and $5e_{1/2}$ sublevels (with approximately four vibrational components in each of the bands) are present in the Auger electron spectrum (AES) of this molecule, see Figs. 1 and 2. Thus a strong decrease of the intensity of the $4e_{1/2}$ Auger resonance is not accidental, and deeper reasons underlying this effect have to be unraveled. The investigation of this problem is also important from the point of view of finding approximate selection rules (propensity rules) for the AES. A preliminary account of some of the results of the present investigation were announced recently [8]. It is the aim of this paper to investigate the mathematical structure of Auger decay of molecular-field-split states in detail and to extend the qualitative discussion made in Ref. [8]. The theory is general, but we nevertheless simplify the presentation by using the H_2S molecule to illustrate its consequences at all stages. The reason for this choice is twofold: H_2S is the simplest possible nondegenerate molecule that possesses all features of the general case, and the clearest experimental results have been obtained for this molecule.

The paper is organized as follows. A qualitative description of the strong depression of the molecular-field-split sublevels in Auger spectra is given in Sec. II and exemplified by the $4e_{1/2}$ resonance in H_2S . An investigation of the S $L_{II,III}$

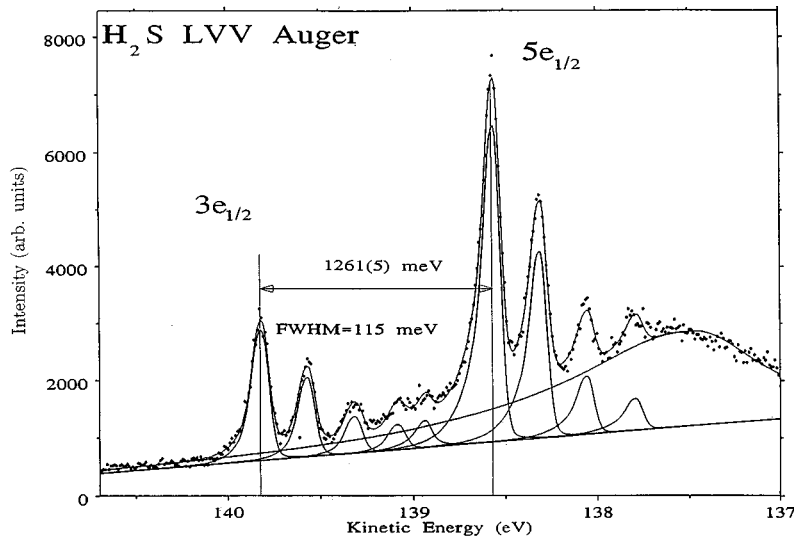


FIG. 1. Experimental LVV Auger spectrum of H_2S . From Ref. [8].

shell accounting for molecular-field and spin-orbit interaction is presented in Sec. III. In the subsequent section, Sec. IV, the cross sections of Auger and photoionization processes are evaluated. The qualitative differences between Auger and photoelectron spectra are discussed in Sec. V. In particular, the strong depression of the $4e_{1/2}$ band in the Auger spectrum in comparison with the photoelectron spectrum of H_2S is shown. The influence of the strong sublevel depression in nonradiative decay on the lifetime of core-excited states is qualitatively discussed in Sec. VI, again using the $3e_{1/2}$, $4e_{1/2}$, and $5e_{1/2}$ sublevels of H_2S for illustration. In the last section, Sec. VII, our findings are discussed and summarized.

II. QUALITATIVE DESCRIPTION OF STRONG DEPRESSION OF THE $4e_{1/2}$ RESONANCE IN THE H_2S AUGER SPECTRUM

We consider first on a qualitative level the most salient feature of the photoionization and Auger spectra of H_2S , namely, the apparent difference of the spin-orbit splitting of the $2p$ level. In the experiment of Ref. [8] the $L_{\text{II,III}}$ electron is ionized to the state $\psi_{\mathbf{k}}$ with energy $\epsilon_{\mathbf{k}}$ by 187-eV photons. The $L_{\text{II,III}}$ hole is annihilated by an electron transition from

the occupied $2b_1$ molecular orbital (MO) with a simultaneous ejection of the second (Auger) electron from the $2b_1$ MO into the continuum state $\psi_{\mathbf{p}}$. The amplitude of this Auger process [9,10],

$$F \propto \alpha^{1/2} \sum_j \frac{\langle \psi_j | \mathbf{d} \mathbf{e} | \bar{\psi}_{\mathbf{k}} \rangle [\psi_{2b_1} \bar{\psi}'_{2b_1} | \psi_j \bar{\psi}_{\mathbf{p}}]}{\omega - (\epsilon_{\mathbf{k}} - E_j) + i\Gamma_j}, \quad (1)$$

induced by an x-ray photon with frequency ω and polarization vector \mathbf{e} , is proportional to the Coulomb integral

$$\begin{aligned} & \langle \psi(2b_1) \psi(2b_1) | \psi_j \psi_{\mathbf{p}} \rangle \\ &= \int \psi_{2b_1}^*(\mathbf{r}_1) \psi_{2b_1}^*(\mathbf{r}_2) \frac{1}{r_{12}} \psi_j(\mathbf{r}_1) \psi_{\mathbf{p}}(\mathbf{r}_2) d\mathbf{r}_1 d\mathbf{r}_2, \quad (2) \end{aligned}$$

where

$$[\psi_1 \psi_2 | \psi_3 \psi_4] = \langle \psi_1 \psi_2 | \psi_3 \psi_4 \rangle - \langle \psi_1 \psi_2 | \psi_4 \psi_3 \rangle. \quad (3)$$

ψ_j and E_j are the wave function and the energy of sublevel j of the $L_{\text{II,III}}$ shell. The one-particle continuum wave function

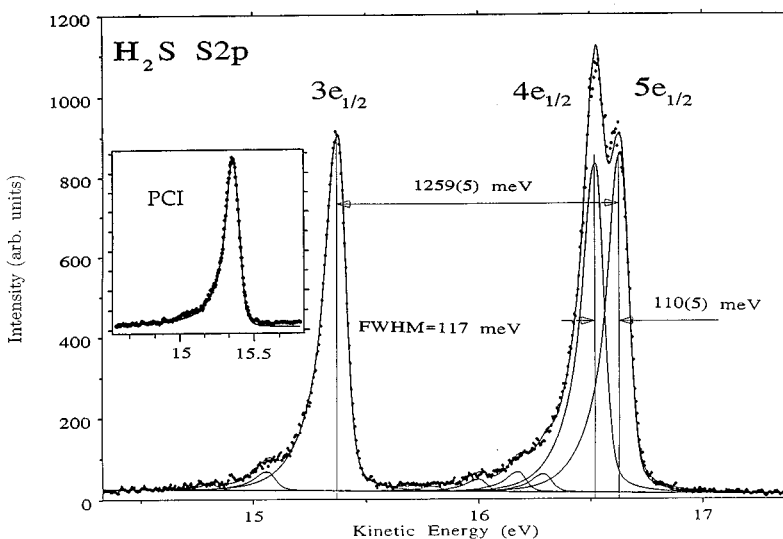


FIG. 2. Experimental S $2p$ photoelectron spectrum of H_2S . From Ref. [8].

$\psi_{\mathbf{k}} \equiv \psi_{\mathbf{k}}^-$ satisfies the normalization condition: $\langle \psi_{\mathbf{k}} | \psi_{\mathbf{k}'} \rangle = \delta(\mathbf{k} - \mathbf{k}')$. The minus sign indicates the incoming asymptotic boundary condition of the wave function $\psi_{\mathbf{k}}^-$. The spin orbital $\bar{\psi}_n$ is the product of space wave function $\psi_n \equiv \psi_n(\mathbf{r})$ and spin-wave function α or β . We will use atomic units ($\hbar = m = e = 1$, $\alpha = 1/137$). The half width at half maximum (HWHM) Γ_j is different for the different sublevels E_j of the S $L_{II,III}$ shell. The summation over j and spins of the $2b_1$ electrons are assumed in Eq. (1).

The $2b_1$ MO of π symmetry is oriented along the x axis in the molecular frame with the H_2S molecule lying in the zy plane, the H—H bond parallel to the y axis, and the sulfur atom at the origin. The Coulomb integral (2) has maximum value if the core-hole wave function ψ_j and the $2b_1$ wave function have the same orientation in space. The order of magnitude of this Coulomb integral is approximately ten times smaller if the wave functions ψ_j and $2b_1$ have perpendicular space orientations. The intensity of the Auger transition is thus large if the contribution of the sulfur $2p_x$ atomic orbital (AO) to the ψ_j wave function is large; otherwise the intensity will be small. We show that the contribution of the $2p_x$ AO to the ψ_j wave function of the $4e_{1/2}$ sublevel is very small. So, the small contribution of the $2p_x$ AO into the $4e_{1/2}$ wave function causes the interdiction of the $2b_1 \rightarrow 4e_{1/2}$ Auger transition.

Now we can understand the more general case. The MF (together with the SO interaction) splits the $L_{II,III}$ shell into sublevels ψ_j with the certain orientation in space. Because of the Coulomb integral (2), the intensity of the Auger transition $\psi_n \rightarrow \psi_j$ will strongly depend on the mutual space orientation of the core ψ_j and valence ψ_n MOs. The strong suppression of the Auger transition takes place if these orbitals are orthogonally oriented in the space local to the core.

III. MOLECULAR-FIELD AND SPIN-ORBIT SPLITTING OF THE S $L_{II,III}$ SHELL OF THE H_2S MOLECULE

To obtain the Auger amplitude (1) we need to solve the Schrödinger equation

$$H\psi = E\psi \quad (4)$$

to first get the one-electron wave functions ψ and energies E of the $L_{II,III}$ shell. We distinguish the atomic (sulfur) Hamiltonian H_0 and the molecular-field potential V_M in the one-electron Hamiltonian operator H of the S $L_{II,III}$ shell,

$$H = H_0 + V_M. \quad (5)$$

The spin-orbit interaction V_{SO} for the $L_{II,III}$ shell is included in the atomic Hamiltonian H_0 . The eigenfunctions ($j=1/2$ or $3/2$)

$$|jm\rangle = R(r) \left[\pm \left(\frac{1}{2} \pm \frac{m}{3} \right)^{1/2} Y_{1m-1/2} \alpha + \left(\frac{1}{2} \mp \frac{m}{3} \right)^{1/2} Y_{1m+1/2} \beta \right] \quad (6)$$

of H_0 (with the associated eigenvalues ϵ_j) are the eigenfunctions of the total angular momentum operator ($\mathbf{J} = \mathbf{L} + \mathbf{S}$). Here $m = -j, -j+1, \dots, j-1, j$; upper and lower signs correspond to $j=3/2$ and $j=1/2$, respectively; α and β are spin functions; and $R(r)$ is the normalized radial part of the sulfur

$2p$ AOs. We will use real spherical functions Y_x, Y_y , and Y_z connected with the complex spherical functions Y_{lm} :

$$Y_{10} = Y_z, \quad Y_{1\pm 1} = 2^{-1/2} (iY_y \pm Y_x). \quad (7)$$

The $L_{II,III}$ SO splitting $\Delta_{SO} = \epsilon_{3/2} - \epsilon_{1/2} \approx 1.26$ eV [8] is much larger than the MF splitting $\Delta_M \sim 0.1$ eV [2] for the H_2S molecule:

$$\Delta_{SO} \gg \Delta_M. \quad (8)$$

In the general case the MF potential V_M mixes all atomic states $|jm\rangle$. The condition (8) allows us to neglect the mixing of states with different total angular momentum values: $j=3/2$ and $j=1/2$. We need only account for the mixing of AO states by V_M within the $j=1/2$ and $j=3/2$ spaces. This mixing is defined by the matrix elements $\langle jm | V_M | jm' \rangle$. The calculation of these matrix elements is simplified if we take into account the symmetry of the H_2S molecule of the symmetry of the MF potential: $V_M(x, y, z) = V_M(-x, y, z) = V_M(x, -y, z)$.

A. The $j=1/2$ case ($3e_{1/2}$ resonance)

The atomic states with the different values of angular momentum projection $m=1/2$ and $m=-1/2$ do not interact:

$$\langle \frac{1}{2} \frac{1}{2} | V_M | \frac{1}{2} - \frac{1}{2} \rangle = 0. \quad (9)$$

Therefore the eigenfunction ψ of the Schrödinger equation (4) coincides with the unperturbed one, while the eigenvalue E ,

$$\psi^{(\pm)} = | \frac{1}{2} \pm \frac{1}{2} \rangle, \quad E = \epsilon_{1/2} + V \quad (10)$$

is only shifted relative to the atomic value $\epsilon_{1/2}$ of the average MF potential

$$V = \langle \frac{1}{2} \pm \frac{1}{2} | V_M | \frac{1}{2} \pm \frac{1}{2} \rangle = \frac{1}{3} (V_x + V_y + V_z), \quad (11)$$

where

$$V_i = \int R^2(r) Y_i^2(\hat{\mathbf{r}}) V_M(\mathbf{r}) d\mathbf{r}, \quad i = x, y, z. \quad (12)$$

So, the MF interaction does not remove the degeneracy of the subshell with $j=1/2$ in the limit (8).

B. The $j=3/2$ case ($4e_{1/2}$ and $5e_{1/2}$ resonances)

Contrary to the $j=1/2$ case the molecular field V_M removes partially the degeneracy of the $j=3/2$ subshell. The splitting of this subshell is caused both by the different MF shifts of the states with the different values of m ,

$$\zeta = \langle \frac{3}{2} \pm \frac{3}{2} | V_M | \frac{3}{2} \pm \frac{3}{2} \rangle = \frac{1}{2} (V_x + V_y),$$

$$\xi = \langle \frac{3}{2} \pm \frac{1}{2} | V_M | \frac{3}{2} \pm \frac{1}{2} \rangle = \frac{1}{3} [\frac{1}{2} (V_x + V_y) + 2V_z], \quad (13)$$

and by the off-diagonal matrix elements of V_M :

$$\eta = \langle \frac{3}{2} \pm \frac{3}{2} | V_M | \frac{3}{2} \mp \frac{1}{2} \rangle = \frac{1}{2\sqrt{3}} (V_y - V_x),$$

$$\langle \frac{3}{2} \pm \frac{3}{2} | V_M | \frac{3}{2} \pm \frac{3}{2} \rangle = 0. \quad (14)$$

The symmetry properties of the matrix elements (13) and (14) allow us to seek the solution of the Schrödinger equation (4) for the subshell $j=3/2$ as

$$\psi^{(\pm)} = A | \frac{3}{2} \pm \frac{3}{2} \rangle + B | \frac{3}{2} \mp \frac{1}{2} \rangle, \quad (15)$$

where the coefficients A and B are defined by the secular equation

$$\begin{aligned} A(\tilde{E} - \zeta) - B\eta &= 0, \\ -A\eta + B(\tilde{E} - \xi) &= 0. \end{aligned} \quad (16)$$

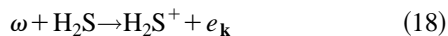
Here $\tilde{E} = E - \epsilon_{3/2}$ is the eigenvalue E of the Schrödinger equation (4) relative to the energy $\epsilon_{3/2}$ of the atomic level with $j=3/2$. Using the normalization condition $\langle \psi^{(\pm)} | \psi^{(\pm)} \rangle = A^2 + B^2 = 1$, we obtain two solutions of Eqs. (16),

$$\begin{aligned} \frac{\tilde{E}_{1,2} - \zeta}{\eta} &= q \pm \sqrt{q^2 + 1}, \quad q = \frac{\xi - \zeta}{2\eta}, \\ A_{1,2} &= \left[1 + \left(\frac{\tilde{E}_{1,2} - \zeta}{\eta} \right)^2 \right]^{-1/2}, \quad B_{1,2} = A_{1,2} \left(\frac{\tilde{E}_{1,2} - \xi}{\eta} \right). \end{aligned} \quad (17)$$

The subscripts 1 and 2 correspond to the signs $+$ and $-$, respectively, on the right-hand side of the first Eq. (17). The solutions $\psi_1^{(\pm)}$ and $\psi_2^{(\pm)}$, (15) and (17), are classified as the Auger resonances $4e_{1/2}$ and $5e_{1/2}$, respectively, while solution (10) describes the $3e_{1/2}$ Auger resonance. The states (15) and (17) of the core shell with $j=3/2$ will be marked below by index $\mu=1,2$: $\psi_\mu^{(\pm)}$, E_μ .

IV. MOLECULAR-FIELD-SPLIT CROSS SECTIONS OF AUGER AND PHOTOIONIZATION PROCESSES

In this section we consider two processes with different mappings of the $L_{II,III}$ shell structure subject to SO and MF interactions. The first one is the photoionization process



of an electron from the S $L_{II,III}$ shell of the H_2S molecule. The Fermi golden rule leads to the following expression for the differential photoelectric cross section for photoionization into the solid angle $d\Omega_{\mathbf{k}}$:

$$\begin{aligned} \sigma^P &\equiv \frac{d^2\sigma^P}{d\epsilon_{\mathbf{k}}d\Omega_{\mathbf{k}}} \\ &= 4\pi^2\alpha\omega \sum_j |\langle \tilde{\psi}_{\mathbf{k}} | \mathbf{e} \mathbf{d} | \psi_j \rangle|^2 \Delta(\omega - (\epsilon_{\mathbf{k}} - E_j), \Gamma_j). \end{aligned} \quad (19)$$

Summation over core-hole states ψ_j and photoelectron spins is then assumed. We introduce here and use below a simplified notation σ for the double-differential cross section. The lifetime broadening of the photoelectron resonance is described by the Lorentzian function

$$\Delta(\omega, \Gamma) = \frac{\Gamma}{\pi(\omega^2 + \Gamma^2)}. \quad (20)$$

After using the solutions (10) and (15) of the Schrödinger equation (4) for the $L_{II,III}$ shell, the photoionization cross section

$$\sigma^P = \sigma_{1/2}^P + \sigma_{3/2}^P \quad (21)$$

near the $3e_{1/2}$ resonance becomes

$$\sigma_{1/2}^P = \frac{8\pi^2\alpha\omega}{3} \sum_{i=x,y,z} |\mathbf{e} \cdot \mathbf{d}_i|^2 \Delta(\omega - (\epsilon_{\mathbf{k}} - E), \Gamma), \quad (22)$$

while the cross section near the $4e_{1/2}$ and $5e_{1/2}$ resonances is

$$\begin{aligned} \sigma_{3/2}^P &= \frac{16}{3}\pi^2\alpha\omega \sum_{\mu=1,2} [a_\mu^2 |\mathbf{e} \cdot \mathbf{d}_x|^2 + b_\mu^2 |\mathbf{e} \cdot \mathbf{d}_y|^2 \\ &+ B_\mu^2 |\mathbf{e} \cdot \mathbf{d}_z|^2] \Delta(\omega - (\epsilon_{\mathbf{k}} - E_\mu), \Gamma_\mu). \end{aligned} \quad (23)$$

Of the two parameters introduced here,

$$a_\mu = \frac{1}{2}(\sqrt{3}A_\mu - B_\mu), \quad b_\mu = \frac{1}{2}(\sqrt{3}A_\mu + B_\mu), \quad (24)$$

one is more important. We will see below that the quantity a_μ defines a strong depression of the Auger transition from the $4e_{1/2}$ hole state. The energies E and $E_\mu = \tilde{E}_\mu + \epsilon_{3/2}$ with $\mu=1,2$ are defined by Eqs. (10) and (17), respectively. Let us remember that the lifetime broadening Γ and the eigenvalue E correspond to the $3e_{1/2}$ resonance, while Γ_1, E_1 and Γ_2, E_2 correspond to the $4e_{1/2}$ and $5e_{1/2}$ peaks in the photoelectron and Auger spectra, respectively. The XPS cross sections (22) and (23) depend on the mutual orientations of the dipole matrix element

$$\mathbf{d}_i = \langle 2p_i | \mathbf{d} | \psi_{\mathbf{k}} \rangle, \quad (25)$$

on the polarization vector \mathbf{e} and on the photoelectron momentum \mathbf{k} . Here $2p_i \equiv R(r)Y_i(\hat{\mathbf{r}})$ is the $2p_i$ AO of the sulfur atom ($i=x,y,z$); $\hat{\mathbf{r}} = \mathbf{r}/r$.

In the second considered process, the Auger process



caused by the absorption of an x-ray photon of frequency ω in accordance with the experimental conditions [8]; the photoelectron $e_{\mathbf{k}}$ has an energy close to the ionization threshold (here $\epsilon_{\mathbf{k}} \sim 10$ eV); while the energy $\epsilon_{\mathbf{p}}$ of the Auger electron is much larger ($e_{\mathbf{p}} \sim 140$ eV). This large energy difference distinguishes these electrons. The double-differential cross section of the Auger electron emission into the solid angle $d\Omega_{\mathbf{p}}$ is expressed through the amplitude (1):

$$\sigma^A \equiv \frac{d^2\sigma^A}{d\epsilon_{\mathbf{p}}d\Omega_{\mathbf{p}}} = \sum \int |F|^2 \Delta(\epsilon_{\mathbf{k}} + \epsilon_{\mathbf{p}} - (2\epsilon_{2b_1} + \omega), \Gamma_f) d\mathbf{k}. \quad (27)$$

Here the summation includes the spins of both the Auger electron and the photoelectrons. The final double-ionized state, here $|2b_1^{-2}\rangle$, is an "optically excited" state and possesses accordingly a small lifetime broadening Γ_f in comparison with the lifetime broadenings Γ or Γ_μ of the inter-

mediate core-excited states $|\psi^{(\pm)-1}\rangle$ or $|\psi_{\mu}^{(\pm)-1}\rangle$. We can therefore replace the Δ function (20) by the Dirac δ function and integrate the right-hand side of Eq. (27) over k . The $2p$ hole states are intermediate states in the Auger process and can therefore interfere. The SO splitting ($\Delta_{\text{SO}}=1260$ meV) is much larger than the lifetime broadening ($\Gamma=35$ meV) [8]. The interference of the Auger scattering channels with $j=3/2$ and $j=1/2$ is therefore negligibly small, and we can write the cross section for the Auger process (27) as

$$\sigma^A = \sigma_{1/2}^A + \sigma_{3/2}^A. \quad (28)$$

It is necessary to mention that the interference of the scattering channels through the intermediate core-hole states with $j=1/2$ and $j=3/2$ may be much more important for other molecules or other spectral transitions than those considered for the H_2S molecule here.

Taking into account the solutions (10), (15), and (17) of the Schrödinger equation for the $L_{\text{II,III}}$ shell and substituting the Auger amplitude (1) into Eq. (27), we can easily prove that the Auger cross section near the $3e_{1/2}$ resonance is

$$\sigma_{1/2}^A = \frac{2\alpha}{9(\Omega^2 + \Gamma^2)} \int |\mathcal{Q}|^2 \sum_{i=x,y,z} |\mathbf{d}_i \cdot \mathbf{e}|^2 d\Omega_{\mathbf{k}}, \quad (29)$$

while the Auger cross sections near the $4e_{1/2}$ and $5e_{1/2}$ resonances are

$$\begin{aligned} \sigma_{3/2}^A = & \frac{8\alpha}{9} \int |\mathcal{Q}|^2 \left[\left| \mathbf{d}_z \cdot \mathbf{e} \sum_{\mu=1,2} \frac{a_{\mu} b_{\mu}}{\Omega_{\mu} + i\Gamma_{\mu}} \right|^2 \right. \\ & + \left| \mathbf{d}_y \cdot \mathbf{e} \sum_{\mu=1,2} \frac{a_{\mu} b_{\mu}}{\Omega_{\mu} + i\Gamma_{\mu}} \right|^2 \\ & \left. + \left| \mathbf{d}_x \cdot \mathbf{e} \sum_{\mu=1,2} \frac{a_{\mu}^2}{\Omega_{\mu} + i\Gamma_{\mu}} \right|^2 \right] d\Omega_{\mathbf{k}}. \quad (30) \end{aligned}$$

Here

$$\begin{aligned} \mathcal{Q} &= \tau \langle \psi_{2b_1}, \psi_{2b_1} | 2p_x \psi_{\mathbf{p}} \rangle, \\ \Omega &= \epsilon_{\mathbf{p}} - (2\epsilon_{2b_1} - E), \quad \Omega_{\mu} = \epsilon_{\mathbf{p}} - (2\epsilon_{2b_1} - E_{\mu}). \quad (31) \end{aligned}$$

The dipole matrix element \mathbf{d}_i (25) depends on the energy $\epsilon_{\mathbf{k}}$ of the photoelectron, which is equal to $\epsilon_{\mathbf{k}} = \omega + 2\epsilon_{2b_1} - \epsilon_{\mathbf{p}}$ in accordance with the energy conservation law, while the Coulomb matrix element \mathcal{Q} depends on the Auger electron energy $\epsilon_{\mathbf{p}}$. All nonessential quantities are collected in the constant τ .

For samples in the gas phase it is necessary to average the cross section (28) over all molecular orientations. This is equivalent to an averaging over the directions of incoming photon propagation under fixed angle θ between the polarization vector \mathbf{e} and the direction \mathbf{p} of the Auger electron propagation. The final result of this averaging is quite unwieldy. Therefore, we present here only the cross section of the Auger process averaged over the directions \mathbf{p} of the Auger electron propagations and over the molecular orientations. This cross section does not differ significantly from the experimental one [8] because in the relevant experiment the principal axis of the electron lens of the spectrometer was

mounted in the so-called pseudomagic angle [$\theta = \arccos(1/\sqrt{3}) \approx 54.7^\circ$] relative to the polarization vector \mathbf{e} of the photon beam. In many cases the cross section measured at this pseudomagic angle is close to the cross section averaged over the \mathbf{p} directions. So, now we need only to average over the \mathbf{e} directions with the help of the formula $e_i e_j = \delta_{ij}/3$. The result of the averaging of the cross sections (29) and (30) over momentum \mathbf{p} and molecular orientations is given by ($\bar{\sigma}^A = \bar{\sigma}_{1/2}^A + \bar{\sigma}_{3/2}^A$)

$$\bar{\sigma}_{1/2}^A = \sigma_0^A \Delta(\Omega, \Gamma) \Gamma^{-1} \quad (32)$$

for the $3e_{1/2}$ resonance, and

$$\bar{\sigma}_{3/2}^A = 2\sigma_0^A \sum_{\mu=1,2} a_{\mu}^2 \Delta(\Omega_{\mu}, \Gamma_{\mu}) \Gamma_{\mu}^{-1} \quad (33)$$

for the $4e_{1/2}$ and $5e_{1/2}$ resonances. Contrary to Eq. (30), the averaged cross section (33) does not contain the term responsible for the interference of scattering channels through the ψ_1 and ψ_2 states. This is a consequence of the orthogonality of these states: $\langle \psi_1 | \psi_2 \rangle = A_1 A_2 + B_1 B_2 = 0$. We used here also the condition of normalization of these states: $A_{\mu}^2 + B_{\mu}^2 = 1$.

To show the qualitative difference between the Auger and photoelectron spectra of the S $L_{\text{II,III}}$ shell we give the final expression for the photoionization cross section (21)

$$\bar{\sigma}^P = \sigma_0^P \left[\Delta(\omega - (\epsilon_{\mathbf{k}} - E), \Gamma) + \sum_{\mu=1,2} \Delta(\omega - (\epsilon_{\mathbf{k}} - E_{\mu}), \Gamma_{\mu}) \right] \quad (34)$$

averaged over molecular orientations and directions \mathbf{k} of the photoelectron propagation. This formula is obtained with the same assumptions as the expression for the cross section of the Auger process, (32) and (33). All quantities in Eqs. (32), (33), and (34) not essential for the discussed problem are collected in the constants

$$\begin{aligned} \sigma_0^A &= \frac{\alpha}{18} \int |\mathcal{Q}|^2 \sum_{i=x,y,z} | \langle 2p_x | d_i | \psi_{\mathbf{k}} \rangle |^2 d\Omega_{\mathbf{p}} d\Omega_{\mathbf{k}}, \\ \sigma_0^P &= \frac{2\pi\alpha\omega}{3} \int \sum_{i=x,y,z} | \langle 2p_x | d_i | \psi_{\mathbf{k}} \rangle |^2 d\Omega_{\mathbf{k}}. \quad (35) \end{aligned}$$

V. ANALYSIS OF EXPERIMENTAL RESULTS

The expressions for the cross sections of photoelectron and Auger spectra were obtained above by assuming an exactly monochromatic x-ray beam. To describe a realistic experimental situation we must use the convolution

$$\tilde{\sigma} = \int_{-\infty}^{\infty} \bar{\sigma}(\omega - \omega') \rho(\omega', \nu) d\omega' \quad (36)$$

of the Auger, (32) and (33), or photoionization (34) cross sections with the total instrumental line profile $\rho(\omega, \nu)$ normalized to unity. The function $\rho(\omega, \nu)$ has a maximum at $\omega=0$. The HWHM ν of the function $\rho(\omega, \nu)$ is defined both by the width of the spectral function of the incoming x-ray photons and by the broadening of the spectrometer. Let us

remember that in the case of Auger spectra we have to use ϵ_p instead of ω in Eq. (36). Now the spectral shapes of Auger ($\tilde{\sigma}^A = \tilde{\sigma}_{1/2}^A + \tilde{\sigma}_{3/2}^A$)

$$\begin{aligned}\tilde{\sigma}_{1/2}^A &= \sigma_0^A \Phi(\Omega, \tilde{\Gamma}) \Gamma^{-1}, \\ \tilde{\sigma}_{3/2}^A &= 2\sigma_0^A \sum_{\mu=1,2} a_\mu^2 \Phi(\Omega_\mu, \tilde{\Gamma}_\mu) \Gamma_\mu^{-1}\end{aligned}\quad (37)$$

and photoelectron spectra

$$\tilde{\sigma}^P = \sigma_0^P \left[\Phi(\omega - (\epsilon_k - E), \tilde{\Gamma}) + \sum_{\mu=1,2} \Phi(\omega - (\epsilon_k - E_\mu), \tilde{\Gamma}_\mu) \right] \quad (38)$$

are described by the convolution

$$\begin{aligned}\Phi(\Omega, \tilde{\Gamma}) &= \int_{-\infty}^{\infty} \Delta(\Omega - \Omega', \Gamma) \rho(\Omega', \nu) d\Omega', \\ \int_{-\infty}^{\infty} \Phi(\Omega, \tilde{g}G) d\Omega &= 1\end{aligned}\quad (39)$$

of the Lorentzian (20) and the total instrumental line profile $\rho(\omega, \nu)$. The last equation is the consequence of a unit normalization of the Δ and ρ functions. The HWHM of the convolution $\Phi(\Omega, \tilde{\Gamma})$ is the function of the widths of the Δ and ρ functions: $\tilde{\Gamma} = \tilde{\Gamma}(\Gamma, \nu)$.

The high-resolution electron spectrum of H₂S [8] demonstrates drastic differences between photoelectron and Auger spectra (see Figs. 1 and 2). The molecular-field splitting of the S $L_{II,III}$ shell into three components, $3e_{1/2}$, $4e_{1/2}$, and $5e_{1/2}$, with comparable intensities was clearly resolved in the photoelectron spectrum of H₂S [8], while only the $3e_{1/2}$ and $5e_{1/2}$ resonances were observed in the LVV Auger spectrum [8] of this molecule. To understand such a strong depression of the $4e_{1/2}$ resonance in the Auger spectrum, let us compare the ratios of the $4e_{1/2}$ and $5e_{1/2}$ intensities in the Auger cross section (37),

$$\frac{\tilde{\sigma}_{3/2}^A(4e_{1/2})}{\tilde{\sigma}_{3/2}^A(5e_{1/2})} = \frac{a_1^2}{a_2^2} \frac{\Gamma_2 \tilde{\Gamma}_2}{\Gamma_1 \tilde{\Gamma}_1}, \quad (40)$$

and in the photoelectron cross section (38),

$$\frac{\tilde{\sigma}^P(4e_{1/2})}{\tilde{\sigma}^P(5e_{1/2})} = \frac{\tilde{\Gamma}_2}{\tilde{\Gamma}_1}. \quad (41)$$

The main factor responsible for the depression of the $4e_{1/2}$ resonance in the Auger spectrum is a_1^2/a_2^2 . This factor is depicted in Fig. 3(a) as a function of q , with the help of Eqs. (17) and (24). It has the order of magnitude $<10^{-1}$ in the region $0 < q < 2$, which is an important result of the present study. The *ab initio* calculation of the molecular-field splitting of the $2p$ shell of H₂S in Ref. [2] confirms that the parameter q resides in this region (see also Table I). In Ref. [2] the MF split ionization potentials I^2B_1 , I^2A_1 , and I^2B_2 of the $2p$ shell were evaluated without taking into account spin-orbit interaction. One can show that parameter q (17) relates to the $2p$ ionization potentials as

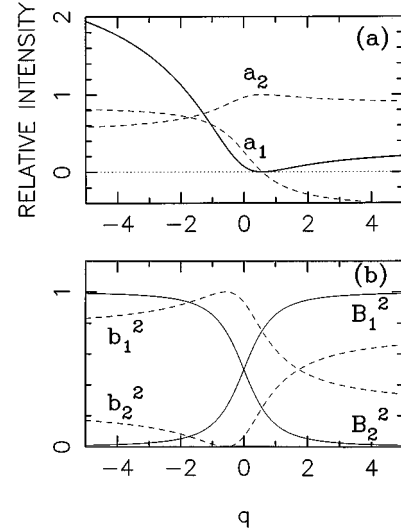


FIG. 3. (a) The dependence of the ratio of intensities of $4e_{1/2}$ and $5e_{1/2}$ Auger resonances, a_1^2/a_2^2 (40) on the parameter q (17) when $\Gamma_2 \tilde{\Gamma}_2 = \Gamma_1 \tilde{\Gamma}_1$ (solid line); the dependences of a_1 and a_2 (24) on q (dashed lines). (b) The q dependences of b_μ^2 (24) (dashed lines) and B_μ^2 (17) (solid lines).

$$q = \frac{2}{\sqrt{3}} \frac{I^2A_1 - 0.5[I^2B_1 + I^2B_2]}{I^2B_2 - I^2B_1}. \quad (42)$$

Table I collects values of the parameter q for five sets of *ab initio* data [2]. To connect Eq. (40) and Fig. 3 with the qualitative explanation for the suppression of the $4e_{1/2}$ resonance given in Sec. II, let us note that a_1 and a_2 are the contributions of the sulfur $2p_x$ AO into the core MOs ψ_1 and ψ_2 of the $4e_{1/2}$ and $5e_{1/2}$ states, respectively.

The experimental Auger spectrum (Fig. 1) shows that the ratio $S^{3/2}/S^{1/2}$ of integral intensities of core subshells with $j=3/2$ and $j=1/2$ is close to 2.5. The theoretical value for this ratio can be obtained indirectly from Eqs. (32) and (33):

$$\frac{S^{3/2}}{S^{1/2}} = \frac{\int \tilde{\sigma}_{3/2}^A d\epsilon_p}{\int \tilde{\sigma}_{3/2}^A d\epsilon_p} = 2 \left(a_1^2 \frac{\Gamma}{\Gamma_1} + a_2^2 \frac{\Gamma}{\Gamma_2} \right). \quad (43)$$

Equation (38) shows that the analogous ratio of integral intensities $S_p^{3/2}/S_p^{1/2}$ is equal to 2 for the photoelectron spectrum [the experiment (Fig. 2) gives approximately the same value]. To derive integral quantities like S^j , the following properties of the a_μ , b_μ , and B_μ coefficients, (24) and (17), are useful:

$$a_1^2 + a_2^2 = b_1^2 + b_2^2 = B_1^2 + B_2^2 = 1. \quad (44)$$

These sum rules are apparent in Fig. 3, where the q dependences of the a_μ , b_μ , and B_μ coefficients are presented. When the HWHMs of the $3e_{1/2}$, $4e_{1/2}$, and $5e_{1/2}$ states are the same ($\Gamma = \Gamma_1 = \Gamma_2$), we see from Eqs. (43) and (44) [see also Fig. 4(c)] that the intensity ratio

$$\frac{S^{3/2}}{S^{1/2}} = 2 \quad \text{if } \Gamma = \Gamma_1 = \Gamma_2, \quad (45)$$

TABLE I. Calculated vertical ionization potentials I in eV, obtained at different computational levels from Table IV in Ref. [2]. Parameter q (42), branching ratio a_1^2/a_2^2 of Auger $4e_{1/2}$ and $5e_{1/2}$ resonances, ratio of integral photoelectron intensities (43), relative Auger energies $\Delta E = E_2 - E_1$, and nonradiative lifetime broadenings $\Gamma_1, \Gamma_2, \Gamma$ (47) in meV.

$I(^2B_1)$	$I(^2A_1)$	$I(^2B_2)$	q	a_1^2/a_2^2	$S^{3/2}/S^{1/2}$	ΔE	Γ_1	Γ_2	Γ
170.89	171.05	171.09	0.35	0.01	1.64	122	26	42	34
170.76	170.86	170.86	0.58	0	1.63	67	26	42	34
170.35	170.44	170.44	0.58	0	1.63	60	26	42	34
170.87	170.93	170.91	1.15	0.03	1.68	35	27	41	34
170.69	170.74	170.71	2.31	0.11	1.77	29	28	40	34

coincides with the multiplicity ratio. This value differs from the experimental one (2.5) by 20%. In the following section we also make a distinction between the Auger rates Γ , Γ_1 , and Γ_2 . Deviations of experimental intensity ratios from the multiplicity ratios have been observed in many spectra. In the case of photoionization Bagus *et al.* [11] and Shklyava, Mazalov, and Murakhtanov [12] have shown that electron correlation effects are mainly responsible for such disagreements.

VI. LIFETIME BROADENINGS OF THE MOLECULAR-FIELD-SPLIT AUGER RESONANCES

One can expect that the lifetime broadenings Γ_1 and Γ_2 of the $4e_{1/2}$ and $5e_{1/2}$ core-excited states differ because of the

strong suppression of the $4e_{1/2}$ line in the Auger spectrum of H_2S . This argument follows from the small fluorescence yield of core-excited states of light elements and from the fact that their lifetimes mainly are defined by the nonradiative decay channel [9,10]. Therefore, the strong prohibition of the $4e_{1/2}$ Auger decay channel should yield a narrowing of the $4e_{1/2}$ resonance and a broadening of the $5e_{1/2}$ line both in the photoelectron and in the Auger spectra of H_2S . Let us estimate the Auger rates of H_2S using a nonrelativistic first-order treatment. In accordance with Wentzel's ansatz [13] the following expression for the nonradiative width of $j=3/2$ core-hole state (15) is obtained ($\mu=1.2$):

$$\Gamma_\mu = \pi \sum_{nn_1} \int |\langle \bar{\psi}_n \bar{\psi}_{n_1} | \psi_\mu^{(+)} \bar{\psi}_p \rangle|^2 d\Omega_p. \quad (46)$$

Here the summation runs over spins of ejected electrons and spins of occupied spin-orbitals $\bar{\psi}_n$ and $\bar{\psi}_{n_1}$. The same formula is valid for the nonradiative lifetime broadening Γ of the core-hole state $3e_{1/2}$ with $j=1/2$, if index μ and summation over μ are removed from Eq. (46). As one can see from Eq. (46), the nonradiative width is state dependent [13,14]. To estimate the nonradiative lifetime broadenings Γ and Γ_μ , the one-center approximation will be used; that is, only the contribution of sulfur AOs into MOs ψ_n will be taken into account: $\psi_{4a_1} = 3s + \dots$; $\psi_{2b_2} = C_y 3p_y + \dots$; $\psi_{5a_1} = C_z 3p_z + C_3 s + \dots$; $\psi_{2b_1} = 3p_x$. The nonradiative widths Γ and Γ_μ are expressed through the MO coefficients C , C_y , and C_z and the atomic decay rates. Equation (46) results in the following lifetime broadenings of the $3e_{1/2}$ state and of the $4e_{1/2}$ ($\mu=1$) and $5e_{1/2}$ ($\mu=2$) states, respectively:

$$\Gamma = 34 \text{ meV}, \quad \Gamma_\mu = (33a_\mu^2 + 17b_\mu^2 + 18B_\mu^2) \text{ meV}. \quad (47)$$

Here the results ($C=0.52$, $C_y=0.61$, $C_z=0.75$) of *ab initio* calculations of H_2S [15] and the data of McGuire [14] were used, and the small contributions of the atomic integral $\int |\langle 3p_x | 2p_z \psi_p \rangle|^2 d\Omega_p$ were neglected. Taking Eq. (44) into account, one can see that the average HWHM for the states $4e_{1/2}$ and $5e_{1/2}$ coincides with the HWHM of the $3e_{1/2}$ state: $(\Gamma_1 + \Gamma_2)/2 = 34 \text{ meV}$. The q dependence of the Auger rates (47) is depicted in Fig. 4(a). In accordance with this dependence the ratio of the integral intensities $S^{3/2}/S^{1/2}$ (43) is not equal to 2 [dotted line in Fig. 4(c)] and depends on the parameter q , too. This dependence makes the agreement with the experimental value worse: $S^{3/2}/S^{1/2} \approx 2.5$. As was men-

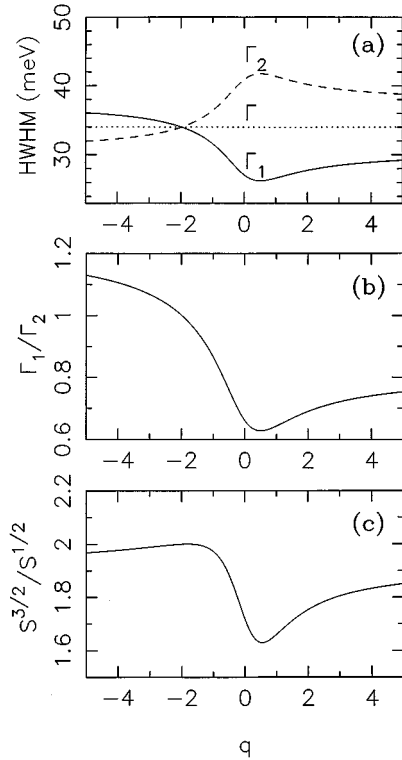


FIG. 4. (a) The dependences of the nonradiative rates Γ (dotted line), Γ_1 (solid line), and Γ_2 (dashed line) (47) of the $3e_{1/2}$, $4e_{1/2}$, and $5e_{1/2}$ resonances on q . (b) The q dependence of the nonradiative width ratio Γ_1/Γ_2 on q . (c) The q dependence of the integral intensity ratio $[S(4e_{1/2}) + S(5e_{1/2})/S(3e_{1/2})]$ (43) with different nonradiative rates (47) (solid line) and with identical nonradiative rates ($\Gamma = \Gamma_1 = \Gamma_2 = 34 \text{ meV}$) (dotted line).

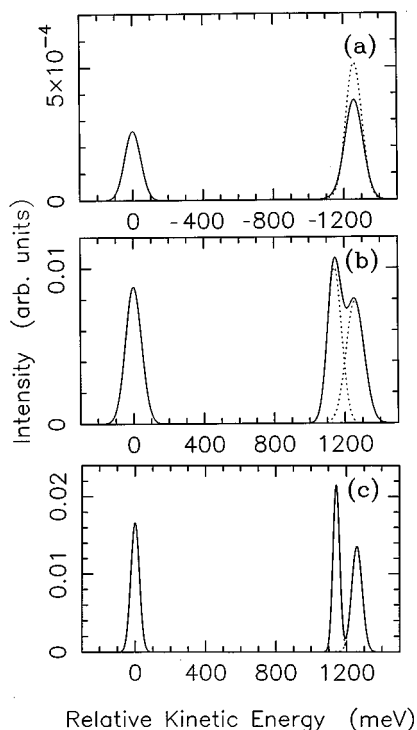


FIG. 5. (a) The LVV Auger spectrum of H_2S as a function of Auger electron energy relative to the $4e_{1/2}$ resonance; $\nu=30$ meV. (b) The $S\ 2p$ photoelectron spectrum of H_2S as a function of photoelectron energy relative to the $4e_{1/2}$ resonance; $\nu=30$ meV. (c) The $S\ 2p$ photoelectron spectrum of H_2S ; $\nu=0$. Spectra depicted by solid lines correspond to different Γ_1 , Γ_2 , and Γ_3 , according to Eq. (47). Dotted lines correspond to the approximation: $\Gamma=\Gamma_1=\Gamma_2=34$ meV. Others are obtained from the first row of Table I.

tioned in the preceding section, the main reason for this disagreement is the restriction to the one-particle model.

We evaluated the Auger (37) and photoelectron (38) spectra for the Gaussian convolution function (39) $\Phi(\Omega, \tilde{\Gamma}) = [1/(\tilde{\Gamma}\sqrt{\pi})] \exp(-\Omega^2/\tilde{\Gamma}^2)$ with $\tilde{\Gamma} = \nu + \Gamma$. The first row of Table I was used as input data for these calculations. The theoretical shape of the LVV Auger spectrum of H_2S is shown in Fig. 5(a). Contrary to the photoelectron spectrum [Figs. 5(b) and 5(c)] the $4e_{1/2}$ resonance is not seen in the Auger spectrum [Fig. 3(a)]. The experimental Auger (Fig. 1) and photoelectron spectra (Fig. 2) confirm this result.

We have shown that the constant core-hole lifetime broadening breaks down when spin-orbit interaction and MF splitting simultaneously are taken into account. In accordance with Eq. (41) the ratio of photoelectron intensities for the $4e_{1/2}$ and $5e_{1/2}$ resonances is equal to 1, if these states have the same lifetime broadening ($\Gamma_1 = \Gamma_2$). But the ratio Γ_1/Γ_2 is not constant and depends strongly on q [Fig. 4(b)]. As indirectly seen from Figs. 5(b) and 5(c) the difference between Γ_1 and Γ_2 is caused by the dependence of the shape of the photoelectron spectra on the width ν of the incoming radiation spectral function [Figs. 5(b) and 5(c)]. Indeed, the intensity ratio of $4e_{1/2}$ and $5e_{1/2}$ resonances in the photoelectron spectrum depends on ν ; it goes as $(\nu + \Gamma_2)/(\nu + \Gamma_1)$.

VII. DISCUSSION

We have outlined a theory for nonradiative decay of molecular-field-split states. The consequences of this theory have been illustrated using spectra of the H_2S molecule. Several findings emerge from the theory. The controversy of the apparent mismatch of L -shell spin-orbit splitting as obtained by photoelectron and Auger spectroscopy is resolved. It is shown that the relative inner-shell sublevel cross sections are very dependent on the matching of spin-orbit and molecular-field interactions. Although the molecular-field splittings for the $2p$ shell of H_2S are only in the range of 10 meV, with the spin-orbit splitting approximately 1 eV, the effect is a complete suppression of one sublevel, the $4e_{1/2}$ level, in the Auger spectrum. This effect, caused by the interplay of spin-orbit and molecular-field interactions, is sensitive to the mutual orientation of initial- and final-state orbitals. We can expect this to be even more pronounced for Raman Auger spectra of penultimate shells of higher-row molecules, such as those recently recorded of M - and N -Auger spectra of, respectively, third-, and fourth-row molecules [5–7].

According to the local propensity rules [16,17] (for a recent study see, e.g., Ref. [18]), the Auger intensities reflect total or orbital charge populations at the site of the core hole. The guiding equations convolute atomic rates by molecular expansion coefficients, with summations of atomic vector coupling coefficients referring to all possible l and m_l quantum numbers. The present analysis indicates, however, that this procedure must be restricted to cases with $l=0$ core-hole states. Indeed, the propensity rules have almost exclusively been used for K spectra of first-row molecules. For L and M spectra involving core-hole states of non- s character, the local Auger intensity expressions should be modified to take account of the molecular-field alignment of this state, restricting the atomic summations over l, m_l values accordingly. The generalization of the propensity rules and the corresponding rate expressions will be given later.

Concerning high-resolution studies, one can anticipate that the alteration of widths and rates by spin-orbit and molecular-field interactions will be even more significant in cases with vibronic excitations stronger than those present in the Auger spectrum of H_2S (in this work we investigate band intensities integrated over vibrational sublevels). Vibronic channel interference will have an increased role, especially in cases in which excitations of more than one vibrational mode are present. The analysis of such cases with nonradiative spectroscopy will require very accurate information on width and form of the excitation energy function. Another aspect that may become relevant is the alteration of the partial and total Auger rates with respect to internuclear conformation. In the molecular-field-split spectra, we anticipate this to be important because of the close proximity of the split levels and because of the high sensitivity of both total and partial rates on the splitting energy. More experimental and theoretical studies of these particular aspects of molecular-field-split Auger spectroscopy can be anticipated in the future.

ACKNOWLEDGMENT

This work was financially supported by a grant from the Swedish Institute (F.Kh.G.).

- [1] S. Svensson, A. Naves de Brito, M. P. Keane, N. Correia, and L. Karlsson, *Phys. Rev. A* **43**, 6441 (1991).
- [2] A. Cesar, H. Ågren, A. Brito, P. Baltzer, M. Keane, S. Svensson, L. Karlsson, P. Fournier, and M. Fournier, *J. Chem. Phys.* **93**, 918 (1990).
- [3] Z. F. Liu, G. M. Bancroft, K. H. Tan, and M. Schachter, *J. Electron Spectrosc. Relat. Phenom.* **67**, 299 (1994).
- [4] B. Wannberg, S. Svensson, M. P. Keane, L. Karlsson, and P. Baltzer, *Chem. Phys.* **133**, 281 (1989).
- [5] J. N. Cutler, G. M. Bancroft, and K. H. Tan, *J. Phys B* **24**, 4897 (1991).
- [6] L. Karlsson, S. Svensson, P. Baltzer, M. Carlsson-Göthe, M. P. Keane, A. Naves de Brito, N. Correia, and B. Wannberg, *J. Phys B* **22**, 3001 (1989).
- [7] L. Karlsson, S. Svensson, P. Baltzer, A. Naves de Brito, N. Correia, and B. Wannberg, *J. Phys B* **24**, L589 (1991).
- [8] S. Svensson, A. Ausmees, S. J. Osborne, G. Bray, F. Gel'mukhanov, H. Ågren, A. Naves de Brito, O.-P. Sairanen, A. Kivimäki, E. Nömmiste, H. Aksela, and S. Aksela, *Phys. Rev. Lett.* **72**, 3021 (1994).
- [9] H. Ågren, A. Cesar, and C.-M. Liegener, *Adv. Quantum Chem.* **23**, 1 (1992).
- [10] T. Åberg and B. Crasemann, in *X-ray Resonant (Anomalous) Scattering*, edited by G. Materlik, K. Fischer, and C. Sparks (Elsevier, New York, 1993).
- [11] P. S. Bagus, M. Schrenk, D. W. Davis, and D. A. Shirley, *Phys. Rev. A* **9**, 1090 (1974).
- [12] N. A. Shklyaeva, L. N. Mazalov, and V. V. Murakhtanov, *J. Struct. Chem.* **20**, 733 (1979).
- [13] G. Wentzel, *Z. Phys.* **43**, 521 (1927).
- [14] E. J. McGuire, *Phys. Rev. A* **3**, 587 (1971).
- [15] F. P. Boer and W. N. Lipscomb, *J. Chem. Phys.* **50**, 989 (1969).
- [16] H. Siegbahn, L. Asplund, and P. Kelfve, *Chem. Phys. Lett.* **35**, 330 (1975).
- [17] H. Ågren, *J. Chem. Phys.* **75**, 1267 (1981).
- [18] F. P. Larkins, J. McColl, and E. Z. Chelkowska, *J. Electron Spectrosc. Relat. Phenom.* **67**, 275 (1994).